Artificial Life and Robotics
https://doi.org/10.1007/s10015-022-00739-w

ORIGINAL ARTICLE

Radiodermatitis grade estimation by RGB color imaging

Ignacio Verdugo-Naranjo[1] · Ana Carolina Hamamura[2] · Gustavo Viani Arruda[2] · George Cunha Cardoso[1] · Juliana Fernandes Pavoni[1]

Received: 2 November 2021 / Accepted: 14 January 2022

Abstract
Radiodermatitis is visually evaluated by the Radiation Therapy Oncology Group (RTOG) scoring scheme, using characteristics such as erythema, desquamation, moist and bleeding. However, subjectivity and differences in skin types and melanin content may bias interpretation. This paper describes the use of RGB cameras for radiodermatitis estimation using image processing. We imaged radiodermatitis evolution throughout the treatment of 23 breast cancer radiotherapy patients of all Fitzpatrick skin phototypes. To prevent confounding information from skin fluids and skin reflection, we used cross-polarized imaging. RGB intensity was corrected using white medical tape as a reference. The RGB color as a function of RTOG grade depended strongly on skin phototype. Yet, when patients are grouped into white, brown, and black skin, the normalized RGB colors reveal stable characteristic signatures that uniquely predict RTOG grade for each group. We conclude cross-polarized RGB imaging as proposed is viable to document and estimate radiodermatitis on all skin phototypes.

Keywords Color measurement · Radiodermatitis evaluation · RGB camera sensing · RTOG grade

1 Introduction

In radiotherapy, irradiation of healthy organs near the tumor is unavoidable. One of the organs undesirably irradiated is the skin, which receives a radiation dose-dependent on individual and therapeutical details [1]. Up to 95% of breast cancer radiotherapy patients experience a skin reaction called radiodermatitis [1, 2].

Radiodermatitis can be classified as acute, and late-onset. The acute reaction is a burn injury, and the skin starts to turn red during the treatment (erythema) because of an increase in blood volume in the sub-papillary plexus [3]. The extent of the erythema depends on the dose, field size, fractionation, and beam quality to comply with the plan used to avoid damage to the skin [2]. Late-onset reactions appear months or years after the radiotherapy ends, and can significantly decrease the patient's quality of life [4].

✉ George Cunha Cardoso
gcc@usp.br

[1] Department of Physics, FFCLRP, University of Sao Paulo, Ribeirao Preto, Sao Paulo, Brazil

[2] Department of Medical Imaging, Hematology and Oncology, Ribeirão Preto Medical School, University of Sao Paulo (FMRP-USP), Ribeirao Preto, Sao Paulo, Brazil

Radiodermatitis has been assessed by physicians using a scoring schema jointly proposed in 1995 by the Radiation Therapy Oncology Group (RTOG) and by the European Organization for Research and Treatment of Cancer (EORTC) [5]. Such scoring schema is defined in grades as follows. Grade 0: no skin is damaged; grade 1: follicular, faint or dull erythema, epilation, dry desquamation, decreased sweating; grade 2: tender or bright erythema, patchy moist desquamation, moderate edema; grade 3: confluent, moist desquamation other than skin folds, pitting edema; grade 4: ulceration bleeding and necrosis; and grade 5: death of the patient associated with radiation late effects [5]. Nevertheless, the RTOG evaluation is purely visual, subject to inter-observer variability, and may suffer from bias depending on skin type and melanin content. Quantitative methods for radiodermatitis evaluation have been presented, such as optical assessments [6–8], imaging-based assessments using ultrasound [9, 10], magnetic resonance [11], and digital color photography [12, 13]. However, all techniques presented either require sophisticated equipment [14]. The gold standard method to evaluate radiodermatitis has still been the visual inspection.

In this paper, we show that digital color photography can be used to track and evaluate the evolution of radiodermatitis. We have used an RGB camera aided by polarizing sheets

Published online: 29 January 2022

(to minimize skin reflection), to record images of 23 female breast cancer patients undergoing radiotherapy. RGB intensities have been compared with the radiodermatitis RTOG grade as measured by trained physicians. Results show that RGB imaging can identify RTOG grade, without the help of a color chart for color correction. This enables the determination of radiodermatitis grade using smartphones or other portable cameras, especially for studies of radiodermatitis mitigation strategies or for telehealth applications.

2 Methods

2.1 Participants

The volunteers in this study consisted of 23 female breast cancer patients over 18 years old, undergoing conventional photon radiotherapy, or hypofractionated photon radiotherapy. The patients were treated approximately five times a week to a total dose of 50 Gy in 25 fractions of 2 Gy for conventional radiotherapy (2 patients), or to a total dose of 42.4 Gy in 16 fractions of 2.65 Gy for hypo-fractionated radiotherapy (21 patients). Patients comprised all Fitzpatrick scale phototypes, non-, partial- and total mastectomy, and comprised all breast sizes. Among these characteristics, we would like to highlight we have included patients with light, medium, and dark skin pigmentation (Table 1), unlike previous similar studies in the literature [1, 2, 6]. The patients in the study reached radiodermatitis classified as RTOG grades 1 and 2. (RTOG 1, and RTOG 2, for short).

2.2 Camera and polarizers

RGB images (JPG, 4 × 3k pixels, 5.37 bits/pixel compression) were acquired with a tripod-mounted portable digital camera (Casio EX-10, 12.1 MP, integrated flash). To minimize flash reflection on the air–skin interface, and to assure imaging of subepithelial layers, light polarizing films were positioned on the camera flash, and on the lens. The polarizing films were cut with scissors to fit the camera flash and camera lens and positioned optically orthogonal to each other. This is a configuration that minimizes camera flash visibility on the image when a mirror is photographed. The polarizers consisted of right-handed circular polarizing films (parallel transmission: 35%; crossed transmission: 0.5%; Polarizing efficiency: 99.98%; retardation film: 125 nm; thickness: 0.28 mm).

For RGB light intensity correction between different images, we used a patch of white waterproof medical tape (FMRP medical tape, white in the visible spectrum, as verified by a portable spectrophotometer). The white medical tape must not have fluorescent whitening agents, which can be easily identified with a UV flashlight. The same package of white waterproof medical tape was used throughout this study. The patch of tape is placed close to the radiotherapy area, avoiding sensitive regions. The typical white patch placement on the patient can be seen in Fig. 1.

2.3 Image acquisition

Patients were imaged on the first day of treatment, in their medical return, and also on pre-scheduled days throughout the treatment. Figure 2 shows the image acquisition days for one of the hypofractionated patients. Consecutive fractions (*fx*) are not necessarily in consecutive days because of pauses on weekends and holidays.

For each imaging session, the patient was seated in an upright position on a stool against a wall. The images were taken in a windowless room next to the radiotherapy room. There, permanent marks placed on the floor and walls ensured same tripod and camera placement between sessions. Patients were shown images of the first day's pose to facilitate reproduction of sitting and arms positions. Small differences in the images could still be found on different days because of patient breathing, and because some debilitated patients had difficulty maintaining the same positions for more than a few seconds after a few sessions of

Table 1 Volunteer patients' phototypes

Fitzpatrick phototype	Total Number of patients	Patients reaching RTOG grade 1	Patients reaching RTOG grade 2
I or II	14	14	4
III or IV	6	6	2
V or VI	3	3	2

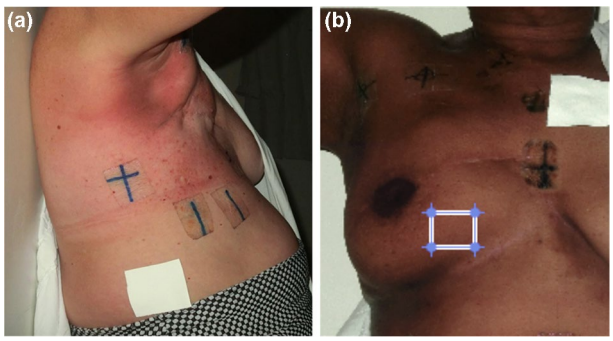

Fig. 1 Illustrative patients' images produced with crossed polarized imaging. **a** Lateral image of a patient with Fitzpatrick skin type I or II. Notice the radiotherapy area that appears with RTOG grade 1. **b** Frontal image of a patient with Fitzpatrick skin type V or VI. Notice a rectangle used as a region of interest (ROI) for radiodermatitis on the right breast of the patient. White patches of medical tape for RGB pixel-level normalization can be observed in both images

Fig. 2 Timeline of radiotherapy for one specific patient. *N fx* represents the *N*th radiation fraction of a hypofractionation schedule. The first and second patient returns after the end of the radiotherapy are also shown. The radiation sessions are conducted on different days, not necessarily consecutive. Each camera icon and arrow points to a fraction (*fx*) on which day a picture was taken. All patients were photographed immediately after the first *fx* and at the 1st return at the end of the treatment. The remaining photographs were taken at random pre-scheduled intermediate treatment days, thus varying from patient to patient

radiotherapy. After lights were turned off, frontal and lateral images (Fig. 1) of the breast undergoing radiotherapy were produced. For comparison with image information, patients were RTOG-graded by two radiation oncologists who reached consensus in all cases.

2.4 Image processing

To carefully track the color of regions of interest (ROI) in the images taken throughout the length of the radiotherapy, we co-registered images of different sessions using affine transformations. As mentioned before, despite careful positioning, a patient presents slight postural changes between sessions. For image registration, we took advantage of anatomical regions, skin marks, and tattoos near the border of the treatment field on the patients. Three of such reference points are necessary for the affine transformation. These reference points were chosen manually in the images taken before the start of radiotherapy. In all other images of the same patient and taken from the same perspective, the corresponding moving points were matched to the reference points via an affine transformation (MATLAB 2015b script for affine transformation using function fitgeotrans).

Among the successfully co-registered images, for each patient pose (frontal or lateral), we chose good images corresponding to days on which the skin in areas undergoing radiotherapy had been identified as having RTOG 0, RTOG 1, and RTOG 2 if available. The ROIs were chosen as regions at which the RTOG had reached the highest grade at the end of the treatment and: (i) was close to the reference points, (ii) showed at least an RTOG grade 1, as evaluated by the physicians, and (iii) did not change drastically along with treatment (deformation, edema). Thus, the ROI position and its size varied from patient to patient, depending on the region being treated and on the extension of the area of radiodermatitis. The co-registration allowed for the automatic selection of corresponding ROIs in earlier images of the same patient. Figure 1b shows a typical ROI, which was selected because that area became RTOG 2 at the end of the treatment. To overcome possible distortion due to skin folding, only the best pictures were chosen and the ROI is smaller than the treated region. In addition, we used the median RGB values instead of the means, to minimize the effect of outlying points. A MATLAB script was written to determine the median pixel intensity level for each RGB channel for the ROIs.

A similar affine transformation was performed with the white patches in the images. The median pixel intensity levels for the white patches in each image were labeled ROI_W (W for white), with corresponding RGB channels: R_W G_W B_W. Normalization of the ROI by the ROI_W for each channel (R/R_W, G/G_W, B/B_W) corrects possible day-to-day variations of camera flash intensity in the RGB channels due to changes in camera exposure time, battery state, and possible changes in patient's arms positioning. Because the use of crossed polarizers minimizes reflections on the surface of the skin, and of the patch, we expect variations due to changes in the angle of incidence of the flash illumination to be negligible.

3 Results and discussion

To study the evolution of skin RGB color throughout radiotherapy, the patients' images were divided into three groups, corresponding to Fitzpatrick phototypes I and II (white skin), III and IV (brown skin), and V and VI (black skin). RGB color response for each Fitzpatrick phototype group is shown in Fig. 3. Notice that the different phototype groups have low standard deviation within a group, but distinct evolution patterns among the groups. We suspect the different evolutions are due to the different responses of melanocytes for the different skin color groups. For example, in Fig. 3c, we notice that for RTOG grade 0, the normalized RGB intensity (above 0.80) is comparable to the corresponding intensity in Fig. 3b. That is, the normalized intensity for RTOG grade 0 is about the same for black and brown skin. Melanin production in skin areas with low exposure to sunlight does not differ significantly between black and brown individuals, because it depends on personal dressing and sun exposure habits. Thus, skin reflectivity ranges among different phototype groups superpose [15]. However, the potential for melanin production once exposed to radiation, always higher in black than brown individuals. Compare Fig. 3b with Fig. 3c for RTOG 1 and 2.

As discussed earlier, the RTOG radiodermatitis scale is not based solely on skin color, but also on the overall aspect of the skin. Yet, taking into account skin phototype, and using polarized photography, our study has shown that radiodermatitis can be graded using color photography. The photographic method also reduces over-reliance on skin

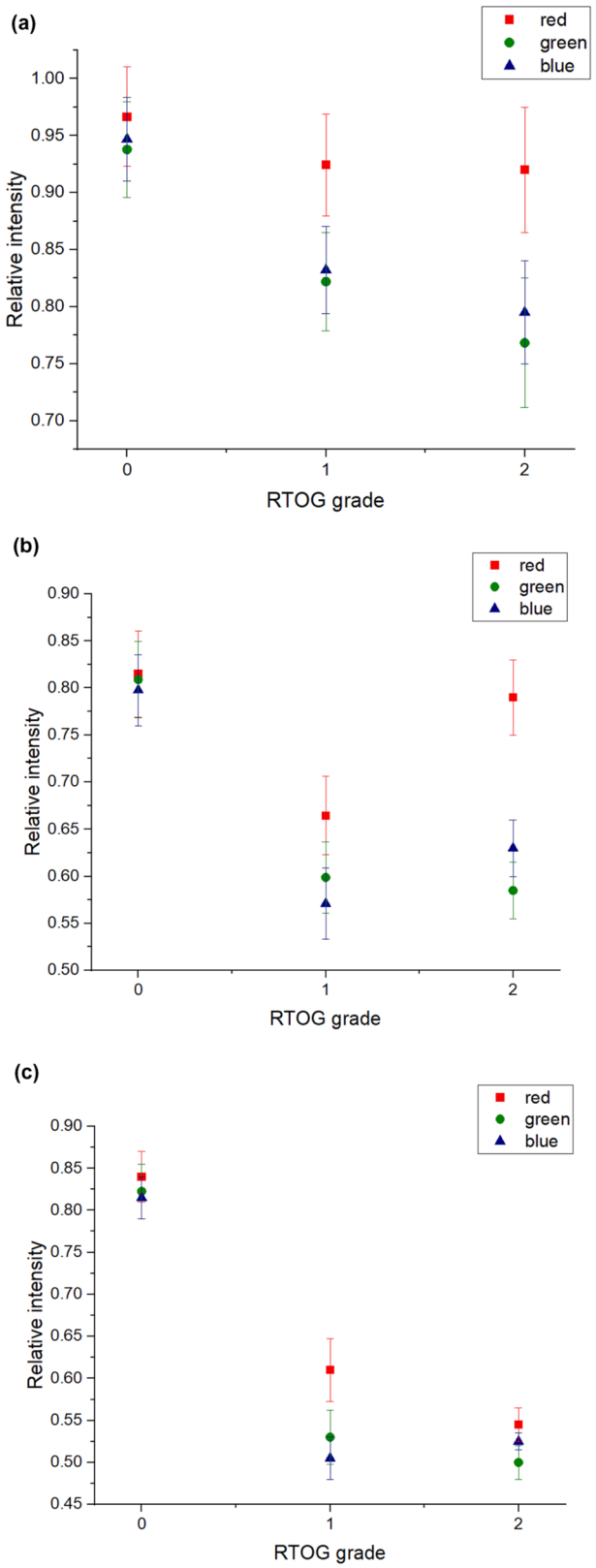

Fig. 3 Normalized RGB values for different phototypes. **a** Fitzpatrick phototypes I, II (white skin); **b** Fitzpatrick phototypes III and IV (brown skin); **c** Fitzpatrick phototypes V and VI (black skin). Notice distinctively different behavior among the different skin color groups, but small standard deviations within the same group

Table 2 Paired *t* test *p* values for the effect of radiodermatitis on independent RGB channels, as shown in Fig. 3

	R	G	B
White skin			
RTOG 0 vs. 1	0.06	**0.0003**	**0.0002**
RTOG 1 vs. 2	0.7	0.9	1.0
Brown skin			
RTOG 0 vs. 1	0.07	**0.003**	**0.0011**
RTOG 1 vs. 2	0.6	0.6	0.6
Black skin			
RTOG 0 vs. 1	**0.02**	**0.002**	**0.002**
RTOG 1 vs. 2	0.18	0.12	0.12

Statistical significance better than 5% is shown in boldface. For the difference in effect between RTOG 1 and RTOG 2 RGB values, the *p* values are high due to the very small number of samples (2 or 4 samples)

erythema (redness) [2]. The difficulty in observing erythema in black patients has been well-discussed in the literature [16]. Our RGB analysis agrees with our expectation that the erythema is more prominent in RTOG grade 2 radiodermatitis of white patients (Fig. 3a). Such redness is not observed in black patients (Fig. 3c). In black patients, despite the lack of observation of erythema, imaging still enables RTOG grading, because the simultaneous observation of all RGB channels gives a clear signature of the radiodermatitis grade that is different for each skin color group.

To investigate the statistical significance of single RGB channel intensity dependence on RTOG grade, we conducted paired *t* tests with the data, as shown in Fig. 3. Table 2 summarizes the statistical results. For white and brown skins, both G and B channels' normalized reflectivity showed very statistically significant results for RTOG 0 to 1 radiodermatitis grades. The red channel changed less. Notice from Fig. 3 that the skin becomes reddish not by an increase in redness, but by a decrease in the reflectivity of green (G) and blue (B) light. For black skin, changes in color saturation between RTOG 0 and RTOG 1 were significant for all RGB channels. In addition, black skin had a larger RGB color change effect, as expected because of the black skin's ability to produce melanin in response to radiation.

For changes between RTOG grades 1 and RTOG 2, changes in single RGB channels can be observed but we could not observe a statistical significance. Here, the small number (4 or 2) of patients reaching RTOG 2 contributes to the lack of statistical significance in the paired *t* test. Still, we verify in Fig. 3 that white and brown skin turn red for RTOG grade 2, once the G and B components become relatively lower than the R component. On the other hand, for black skin, for RTOG 2, the intensities of the R, G, and B components drop simultaneously, which turns the skin darker, not reddish (erythema). This observation is in line

with the expected difficulty in observing erythema in black patients [16].

Earlier studies on the use of RGB cameras in grading radiodermatitis [13, 17] have focused on erythema and tested on a limited range of skin phototypes. Our measurements have shown the full range of Fitzpatrick phototypes. In addition, we have used simple equipment, with no color target. For RGB intensity correction, we successfully used a simple white medical tape. Simplicity matters because radiodermatitis can appear long after the end of radiotherapy treatment, and the availability of tools even for the non-specialist encourages evaluation of RTOG grade evolution.

Among the limitations in this study, is the fact we did not collect information about the use or non-use of a radiodermatitis cream between sessions. Patients had been only advised to not use radiodermatitis cream during radiation sessions, because cream increases radiation interaction with the skin. As for the use of cream in between sessions, we do not know the effect on radiodermatitis or modification in skin properties that could confuse RTOG grading. Nevertheless, variability due to cream usage issues is unlikely to have happened in our study, because the RTOG scale was applied by consensus by the two physicians without hesitation. In addition, for each phototype group, RGB values as a function of radiodermatitis have small standard deviations. Another limitation in this preliminary study is that we did not automate the radiodermatitis grade classification. Again, the small standard deviation shown by the RGB metrics of each phototype group presents a clear pattern of evolution of RGB relative values, with radiodermatitis grade. This pattern is especially clear when the RGB values are compared to normal skin's RGB values (Fig. 3).

In a larger study, the simultaneous use of the three RGB channels to describe the evolution of radiodermatitis seems to be ideal. Given that the color evolution of different phototypes differs along with the evolution of radiodermatitis, any evaluation requires identification of the phototype and also a measurement of normal skin (RTOG grade 0). We suggest that a classification of the Fitzpatrick phototypes into three groups, as done in this study, may be sufficient.

As future work, we suggest the use of strategies to digitally separate the melanin chromophores to produce results that are independent of skin phototype. With processing for chromophore separation (melanin image, hemoglobin image) [18] the radiation effect on the skin will be better understood. Alternatively, the oxyhemoglobin and desoxyhemoglobin chromophores could be digitally separated [19] in the images, and the evolution of skin oxygenation can be observed. With current techniques, chromophore separation would require image acquisition with a color target, or a calibrated camera and illuminator.

4 Conclusion

Photographic evaluation of radiodermatitis is possible and can be done for all phototypes. Such imaging technique enables non-specialized medical professionals or even patients to monitor and record skin's RTOG. The technique can be also used for large-scale radiodermatitis cream evaluation for extended periods. In addition, the use of RGB cameras opens up the possibility of smartphone cameras being used to identify radiodermatitis in telehealth and remote medical consultations.

Acknowledgements We thank Dr. Alexandre Faustino, MD, of the Ribeirao Preto Medical School Hospital (University of Sao Paulo) for discussions on the classification of radiodermatitis grades.

Funding This study was financed in part by the Coordenação de Aperfeiçoamento de Pessoal de Nível Superior—Brazil (CAPES)—Finance Code 001. GCC ORCID 0000-0001-8459-9812, JFP ORCID: 0000-0002-1647-8231.

Declarations

Ethics approval This study was approved by FFCLRP/HC-FMRP/University of Sao Paulo Ethics Committee (certificate CAAE 73541017.20000.5407) and complies with the Declaration of Helsinki. All volunteering patients provided informed consent before participation in the study, and no patient received financial compensation for the study.

References

1. Baines CR, McGuiness W, O'Rourke GA (2016) An integrative review of skin assessment tools used to evaluate skin injury related to external beam radiation therapy. J Clin Nurs 26:1137–1144
2. Nystrom J, Geladi P, Lindholm-Sethson B, Larson J, Svensk AC, Franzen L (2008) Objective measurements of radiotherapy-induced erythema. Skin Res Technol 10:242–250
3. Jacques SL, Ramella-Roman JC, Lee K (2002) Imaging skin pathology with polarized light. J Biomed Opt 7(3):329–340
4. Seité S, Bensadoun RJ, Mazer JM (2017) Prevention and treatment of acute and chronic radiodermatitis. Breast Cancer: Targets Ther 9:551
5. Cox JD (1995) Toxicity criteria of the radiation therapy oncology group (RTOG) and the European organization for research and treatment of cancer (EORTC). Int J Radiat Oncol Biol Phys 31:1341–1346
6. Ahmad Fadzil MH, Ihtatho D, Mohd Affandi A, Hussein SH (2009) Objective assessment of psoriasis erythema for PASI scoring. J Med Eng Technol 33(7):516–524
7. Lahti A, Kopola H, Harila A, Myllylä R, Hannuksela M (1993) Assessment of skin erythema by eye, laser doppler flowmeter, spectroradiometer, two-channel erythema meter, and Minolta chroma meter. Arch Dermatol Res 285(5):278–282
8. Sattler EC, Kästle R, Welzel J (2013) Optical coherence tomography in dermatology. J Biomed Optics 18(6):061224
9. Wong S, Kaur A, Back M, Lee KM, Baggarley S, Lu JJ (2011) An ultrasonographic evaluation of skin thickness in breast cancer

patients after postmastectomy radiation therapy. Radiat Oncol 6(1):1–10
10. Warszawski A, Röttinger EM, Vogel R, Warszawski N (1998) 20 MHz ultrasonic imaging for quantitative assessment and documentation of early and late postradiation skin reactions in breast cancer patients. Radiother Oncol 47(3):241–247
11. Querleux B (2004) Magnetic resonance imaging and spectroscopy of skin and subcutis. J Cosmet Dermatol 3(3):156–161
12. Raina A, Hennessy R, Rains M, Allred J, Hirshburg JM, Diven DG, Markey MK (2016) Objective measurement of erythema in psoriasis using digital color photography with color calibration. Skin Res Technol 22(3):375–380
13. Setaro M, Sparavigna A (2002) Quantification of erythema using digital camera and computer-based colour image analysis: a multicentre study. Skin Res Technol 8(2):84–88
14. Abdlaty R, Haywar J, Farrell T, Fang Q (2020) Skin erythema and pigmentation optical assessment techniques. Photodiagn Photodyn Therapy 1:102127
15. Rubegni P, Cevenini G, Flori ML, Fimiani M, Stanghellini E, Molinu A, Barbini P, Andreassi L (1997) Relationship between skin color and sun exposure history: a statistical classification approach. Photochem Photobiol 65(2):347–351
16. Ben-Gashir MA, Seed PT, Hay RJ (2002) Reliance on erythema scores may mask severe atopic dermatitis in black children compared with their white counterparts. Br J Dermatol 147(5):920–925
17. Matsubara H, Matsufuji N, Tsuji H, Yamamoto N, Karasawa K, Nakajima M, Takahashi W, Karube M (2015) Objective assessment in digital images of skin erythema caused by radiotherapy. Med Phys 42(9):5568–5577
18. Tanaka S, Tsumura N (2020) Improved analysis for skin color separation based on independent component analysis. Artif Life Robot 25(1):159–166
19. Mustari A, Kanie T, Kawauchi S, Sato S, Sato M, Kokubo Y, Nishidate I (2018) In vivo evaluation of cerebral hemodynamics and tissue morphology in rats during changing fraction of inspired oxygen based on spectrocolorimetric imaging technique. Int J Mol Sci 19(2):491